



## Characterizing the fracture resistance of proton exchange membranes

Yongqiang Li<sup>a,\*</sup>, Jennifer K. Quincy<sup>a</sup>, Scott W. Case<sup>a</sup>, Michael W. Ellis<sup>b</sup>, David A. Dillard<sup>a</sup>, Yeh-Hung Lai<sup>c</sup>, Michael K. Budinski<sup>c</sup>, Craig S. Gittleman<sup>c</sup>

<sup>a</sup> Department of Engineering Science and Mechanics, Virginia Polytechnic Institute and State University, Blacksburg, VA 24061-0219, United States

<sup>b</sup> Department of Mechanical Engineering, Virginia Polytechnic Institute and State University, Blacksburg, VA 24061-0238, United States

<sup>c</sup> Fuel Cell Research Labs, General Motors Corporation, 10 Carriage Street, Honeoye Falls, NY 14472-1039, United States

### ARTICLE INFO

#### Article history:

Received 11 March 2008

Received in revised form 14 June 2008

Accepted 16 June 2008

Available online 1 July 2008

#### Keywords:

Proton exchange membrane durability

Essential work of fracture

Trouser tear test

Knife slit test

Intrinsic fracture energy

Pinhole formation

### ABSTRACT

Pinhole defects that form in proton exchange membranes (PEMs) due to the cyclic hygrothermal stresses induced during the operation of a fuel cell and cause gas crossover may be interpreted as a result of crack formation and propagation. The goal of this study is to employ a fracture test to approach the intrinsic fracture energy of a perfluorosulfonic acid proton exchange membrane. The intrinsic fracture energy has been used to characterize the fracture resistance of polymeric materials with minimal plastic dissipation and the in absence of viscous dissipation, and has been associated with the long-term durability of polymeric materials where subcritical crack growth occurs under slow time-dependent or cyclic loading conditions. Insights into this limiting value of fracture resistance may offer insights into the durability of PEMs, including the formation of pinhole defects. In order to achieve this goal, a knife slit test which significantly reduces the plastic deformation during the test by limiting the plastic zone size with a sharp blade is conducted. Additionally, double edge notched tension tests and trouser tear tests are conducted to obtain the essential work of fracture and tear energy, respectively. It has been found that although the fracture energy obtained with the knife slit test is still several times larger than the intrinsic fracture energy of regular polymer materials, it is several orders of magnitude lower than those obtained with the other two methods, where process-dependent viscous and plastic dissipation dominate over the intrinsic material property.

© 2008 GM Global Technology Inc. Published by Elsevier B.V. All rights reserved.

### 1. Introduction

Long-term reliability of proton exchange membrane (PEM) fuel cells depends on the long-term electrochemical and mechanical integrity of the PEMs. Over a range of test conditions, small tensile coupons of these membranes often demonstrate considerable ductility, dissipating large amounts of energy and straining to several times their original length [1,2]. Examination of pinhole defects in membranes removed from failed fuel cells often show considerable thinning, presumably resulting from plastic flow of material due to concentrated stresses. In the mean time, these same micrographs reveal cracks that appear to result from relatively brittle crack propagation. Due to the brittle nature of catalyst layers, mud cracks of different depths are typically present in the electrodes. When these cracks reach the electrode–PEM interface, they can cause delamination and/or cracking of the PEM. When the surface cracks in the PEM initiated this way propagate through the thickness, reactant gases can crossover and reduce

the efficiency and eventually halt the operation of the fuel cell [3–5].

Concepts of fracture mechanics may be employed to study the formation of mud cracks in membrane electrode assemblies (MEAs) during manufacturing, storage and handling, cracking behavior at the electrode and PEM interface, crack propagation within a PEM, and interactions of cracks propagating from both sides of a PEM. However, direct application of fracture mechanics is not without challenges. The uniaxial stress–strain response of a PEM shows substantial plastic deformation exhibiting over 100% strain at break [1,2] and common fracture mechanics tests give measured fracture energies on the order of  $20 \text{ kJ m}^{-2}$  or more [6]. Both properties indicate that a typical PEM is highly ductile and the plastic zone ahead of a crack tip is many times larger than the thickness of the membrane. Nevertheless, cracks have been found to propagate into the PEM and cause significant amounts of gas crossover during RH cycling tests with little evidence of macroscopic plastic deformation seen in post-mortem examination. This led us to consider the effect of sustained loading and cyclic fatigue. Refs. [7,8] represent finite element analyses of fatigue stresses in PEMs during RH cycling. Fatigue fracture requires substantially less energy than quasi-static fracture, which

\* Corresponding author. Tel.: +1 585 624 6560; fax: +1 585 624 6680.  
E-mail address: [li233@vt.edu](mailto:li233@vt.edu) (Y. Li).

involves extensive viscous dissipation and plastic deformation. When cracks in the materials propagate at an extremely low rate such that viscous dissipation disappears, the energy cost during the process is called the intrinsic or threshold fracture energy. The existence of the intrinsic fracture energy provides a threshold that governs the fracture of a material under extended static (creep) and/or cyclic fatigue loading. At such energy level, plastic yielding of the material also disappears [9]. To experimentally obtain the intrinsic fracture energy, plastic deformation ahead of the crack tip during a fracture test needs to be minimized. However, reducing plastic deformation is not easy to accomplish during fracture tests of PEMs that are 0.025 mm or thinner, as large scale yielding is often incurred during fracture toughness tests in a plane stress situation [10].

In this study, we evaluated three different testing methods to investigate the fracture response of PEMs: the double edge notched tension (DENT) test for obtaining the essential work of (plane stress) fracture (EWF), the trouser tear test, and a modified knife slit test. Following the experimental details, fracture resistance results obtained from these tests are compared and the advantages of the modified knife slit test over others are discussed. The effect of the cutting angle was studied with the modified knife slit test and a desirable cutting angle associated with minimal frictional effects and plastic dissipation was found.

**2. Experimental details**

**2.1. Materials**

For all experiments, DuPont’s Nafion® NRE-211 membrane was tested as a representative PFSA (perfluorosulfonic acid) PEM. NRE-211 is a non-reinforced, dispersion-cast Nafion® film with a nominal thickness of 0.025 mm. Using a dynamic mechanical analyzer (DMA) [11], the  $\alpha$ -transition temperature of dry Nafion® was found to be around 103 °C, which is slightly higher than the typical operating temperature of PEM fuel cell stacks. In addition, from dry to the fully hydrated state, NRE-211 shows around 60% isotropic hygral expansion in volume and significant stress can develop during RH cycling tests [7,8]. As a result, NRE-211 exhibits relatively poor performance during relative humidity cycling tests [4,5]. This can be interpreted in that NRE-211 is prone to crack formation and propagation during such tests.

**2.2. Double edge notched tension test (DENT)**

The essential work of fracture (EWF) has been widely used as a measure of the fracture resistance of polymeric films [12,13], due to the inability to conduct plane strain fracture tests on thin membranes. The concept assumes that the total fracture energy during the fracture of a pre-cracked specimen can be separated into geometry-independent (essential) work and geometry-dependent (non-essential) work:

$$W_F = W_E + W_P \tag{1}$$

where  $W_F$  is the total work of fracture,  $W_E$  is the essential work that is expended to yield and tear the film within the inner fracture process zone, and  $W_P$  is the non-essential work to yield the outer plastic zone. In a DENT test, the size of the outer plastic zone is proportional to the uncut ligament length, thus the above equation can be rewritten as

$$w_F l t = w_E l t + \beta w_P l^2 t \Rightarrow w_F = w_E + \beta w_P l \tag{2}$$

where  $w_E$  and  $w_P$  are specific works corresponding to the terms in Eq. (1),  $l$  is the length of the uncut ligament length,  $t$  is the

thickness of the specimen, and  $\beta$  is the shape factor of the outer plastic zone. Following Eq. (2),  $w_E$  can be obtained by conducting DENT tests with specimens of different uncut ligament lengths and extrapolating the  $w_F$  vs.  $l$  line to zero  $l$ . The concept of EWF and the fracturing of a DENT specimen made of a reinforced PFSA membrane (to aid visibility) as an example are illustrated in Fig. 1 [5,6]. The DENT specimens used in the present study had a gage length of 70 mm and were 35 mm wide. The length of the uncut ligament ranged from 5 mm to 30 mm. The pre-cracks were cut to length with a microtome blade. The specimen was loaded on an MTS universal testing machine to complete rupture at a crosshead rate of 0.08 mm s<sup>-1</sup> while recording force and displacement.

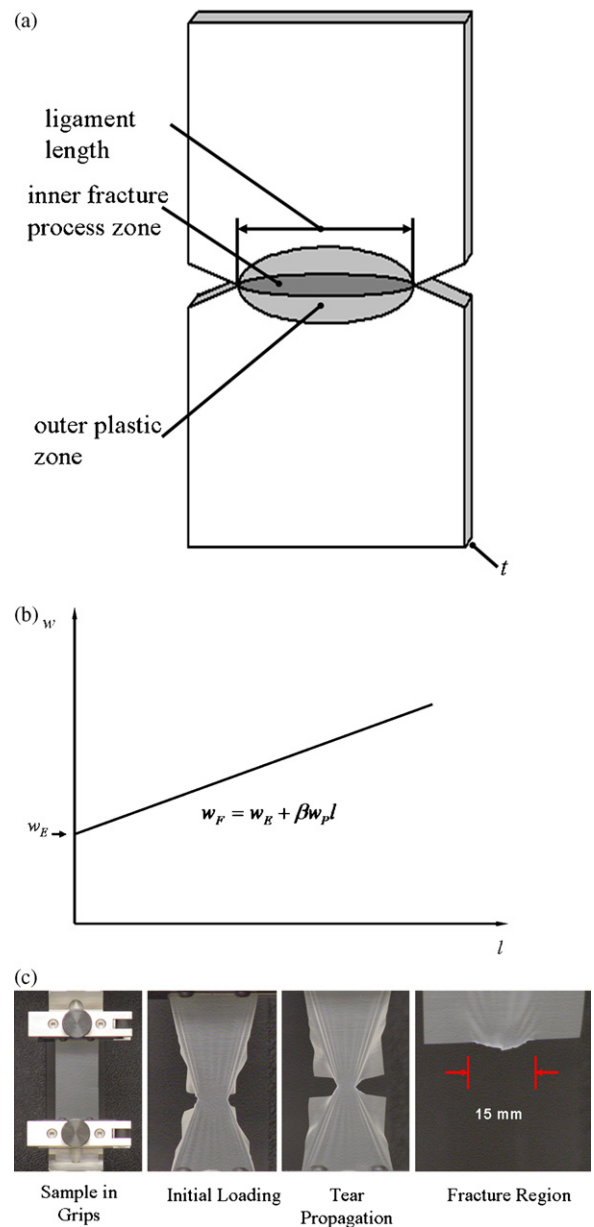


**Fig. 1.** Essential work of fracture and DENT test images: (a) schematic illustration of the inner fracture process zone and the outer plastic zone in the cracking of an in-plane pre-cracked specimen; (b) the linear relationship between the total specific fracture energy  $w_F$  and the uncut ligament length  $l$  [12,13]; (c) the cracking of a DENT sample of a reinforced membrane (for ease of photographing).

### 2.3. Trousers tear test

The trouser tear test (ASTM D 1938 (2002)) [14], schematically shown in Fig. 2 is a simple technique that has been widely used to characterize the fracture energy of ductile plastic and metallic films (up to 0.25-mm thick) and sheets (up to 1-mm thick). This test is easy to conduct and is relatively insensitive to errors in alignment. A strip of membrane is pre-cracked and the two legs are pulled in opposite directions to nominally fracture the uncut ligament with globally mode III loading. Because many materials tested with this method are soft and ductile, the fracture plane rotates and it is no longer perpendicular to the plane of the uncut sheet, resulting in mixed mode loading. But regardless of the mode of fracture, as long as the samples crack in a self-similar way, the total energy expended during a trouser tear test is typically reported as:

$$G_{\text{tear}} = \frac{2(P)}{t} \quad (3)$$

where  $(P)$  is the average force and  $t$  is the thickness of the membrane. The factor of two is due to the fact that when the crosshead moves over a unit distance, the crack extends only half this distance (assuming that the strain in the legs, in the order of 0.001 considering a tearing energy of  $10 \text{ kJ m}^{-2}$  and an elastic modulus of 250 MPa for the PEM, is negligible). There are, however, doubts regarding the correct thickness (or crack area) to use, in that cracks may form at an angle to the normal, representing a wider crack area than the thickness of the membrane. At this time, we have not obtained quantitative measurements of the actual fracture surfaces, and as a result, the fracture energies reported herein should be the upper limit energy.

The geometry of the trouser tear specimen is also shown in Fig. 2. After creating the pre-crack with a microtome blade, the legs were separated and clamped in the MTS testing machine. The trouser tear tests were conducted at different tearing rates at ambient conditions.

### 2.4. Knife slit test

By limiting the plastic dissipation during tearing with the presence of a sharp blade tip, Lake and Yeoh [15] and Gent et al. [16,17] utilized a knife slit test to obtain the tearing fracture energy ( $T$ ) and

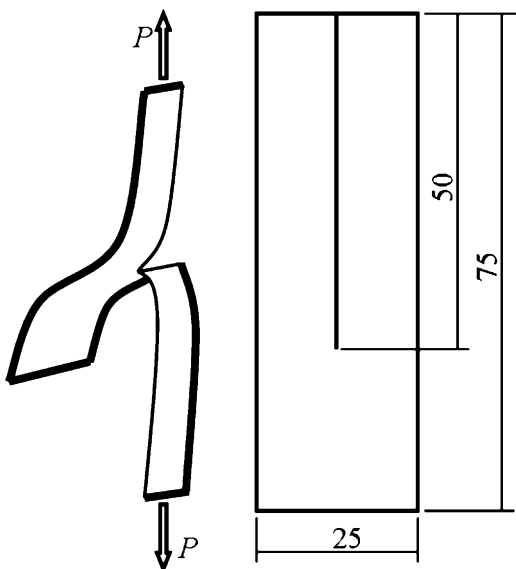


Fig. 2. An illustrative figure of the trouser tear test and the geometry of the trouser tear specimen (unit: mm).

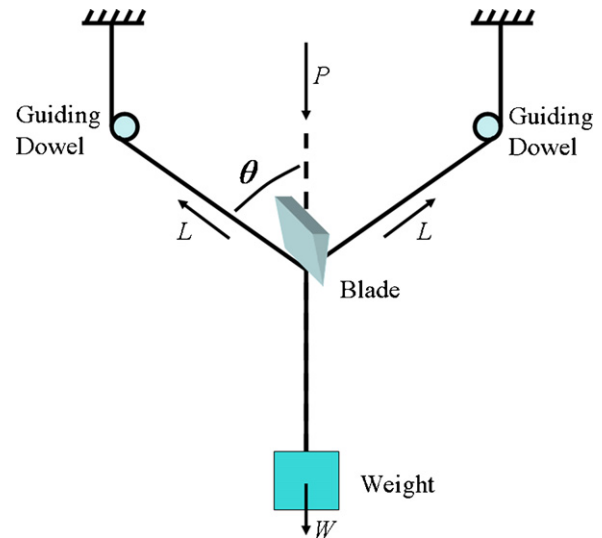


Fig. 3. Schematic illustration and equilibrium diagram of the knife slit test used in this study. The blade and the two guiding dowels remain stationary relative to one another (all moving at the same velocity) such that during the cutting process, the cutting angle  $\theta$  is constant.

cutting fracture energy ( $C$ ) of rubber and plastic sheets. To reduce frictional effect, Lake and Yeoh [15] separated the cracked ligaments apart so that they were not in contact with the faces of the blade, and Gent et al rotated the knife  $45^\circ$  to further minimize the contact area near the crack tip. Interested readers may refer to references [15–17] for details about their test fixtures.

Gent and coworkers found that the effective crack tip diameter inferred from the measured fracture energy for silicone rubber was on the order of the blade radius, and for thermoplastics such as high density polyethylene, the diameter was on the order of one to three times the size of the spherulite structure, which was significantly larger than the blade radius [16]. As the  $C-T$  ratio can be adjusted by separating the legs at different angles or applying different tearing forces, Gent and coworkers were able to examine the effectiveness of their method by plotting the cutting energy against the tearing energy for various materials [16,17]. At a given cutting rate and temperature, the total fracture energy ( $C+T$ ) should remain constant if the test had completely eliminated friction and plastic dissipation during tearing. They found that for silicone elastomers, the  $C-T$  results almost followed the  $C+T = \text{constant}$  line at high cutting energy and low tearing energy; as the fracture inclined toward more tearing mode, the total fracture energy increased. They explained that when  $T$  is too large, tearing took place somewhat ahead of the blade tip and the roughness of the fracturing surface is no longer controlled by the blade tip, which undermines the effectiveness of the blade [17]. Therefore, for a particular material, an optimal slitting configuration that leads to the smallest total fracture energy (thus closest to the intrinsic fracture energy of the material) may be found by splitting the total fracture energy into the correct cutting and tearing components, i.e. reducing the frictional effect by increasing the cutting angle without causing uncontrolled plastic tearing.

The modified knife slit test conducted in the present study is schematically shown in Fig. 3 and a photograph of part of the fixture is shown in Fig. 4. There are mainly two reasons for the modifications made to the aforementioned configurations to better serve the study of PEMs. Firstly, commercial PEMs are very thin and the forces required for cutting and tearing are very small, which can be easily exceeded by frictional forces at the pulleys used in prior configurations. In the modified configuration, the cutting and tear-

ing forces are not affected by friction and can be obtained with an equilibrium analysis. Secondly, we found that the modified configuration can be readily miniaturized and lends itself to easy enclosure in an environment chamber.

Following equations given by Lake and Yeoh [15],  $C$ ,  $T$  and  $G$  (total fracture energy) for the present testing configuration are

$$C = \frac{\lambda P}{t}$$

$$T = \frac{2\lambda L(1 - \cos\theta)}{t} = \frac{\lambda(P + W)(1 - \cos\theta)}{t \cos\theta} \quad (4)$$

$$G = C + T$$

where  $\lambda$  is the average extension ratio in the membrane,  $L$  is the pulling force in each leg,  $P$  is the cutting force,  $W$  is the tearing weight hanging under the uncut ligament,  $\theta$  is the cutting angle and  $t$  is the thickness of the membrane (shown in Fig. 3).

The geometry of the sample is similar to that used in the trouser tear tests (shown in Fig. 2), except that the total length was 305 mm and the pre-crack length was 216 mm. Test samples were mounted in the fixture, as illustrated in Fig. 4. The two legs were separated, passed around the guiding dowels, and connected to the stationary beam on top of a screw-driven Instron machine (where the two small binder clips in Fig. 4 are mounted). The knife (Leica #818 microtome blade) was connected to a 0.5 N Interface Force ULC series 0.5 N load cell, which was mounted on the aluminum frame. To avoid direct contact with the frame, which would be warm in an elevated-temperature test, the load cell was fixed on top of a composite mounting block (dark block in the center of the picture). The aluminum frame sat on the moving crosshead of the screw-driven Instron testing machine, so when it traversed downward, the knife cut through the uncut ligament, which was supported from the top crosshead of the machine.

A chamber, built of polystyrene foam, sat on a scissor jack so that it can be raised to achieve an effective seal with the beam of the frame. Heating pads inside the chamber were used to control the temperature, and saturated salt solutions listed in Table 1 were used to generate different humidity levels in the chamber. Moving the crosshead at different speeds enabled us to collect rate-dependent cutting and tearing energies.

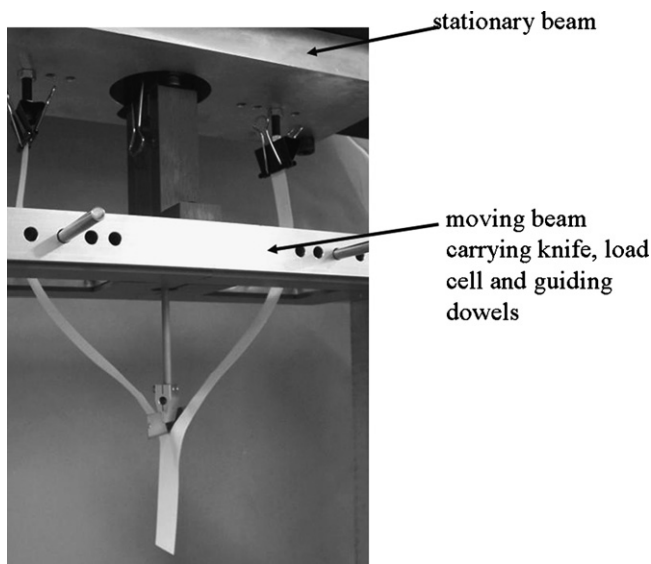


Fig. 4. The test fixture used in this study. By placing the guiding dowels in different holes, tests of different cutting angles can be conducted. A dummy paper sample was loaded in place of a transparent PEM sample for ease of photographing. No weight was hung at the bottom of the sample in this illustrative picture.

Table 1

Saturated salt solutions used to control the humidity in the chamber (ASTM E 104-02 [14])

Salt	RH (%)
Lithium chloride (LiCl)	11
Magnesium chloride (MgCl <sub>2</sub> )	35
Magnesium nitrate (Mg(NO <sub>3</sub> ) <sub>2</sub> )	55
Sodium chloride (NaCl)	75
Potassium chloride (KCl)	85
None (pure water)	100

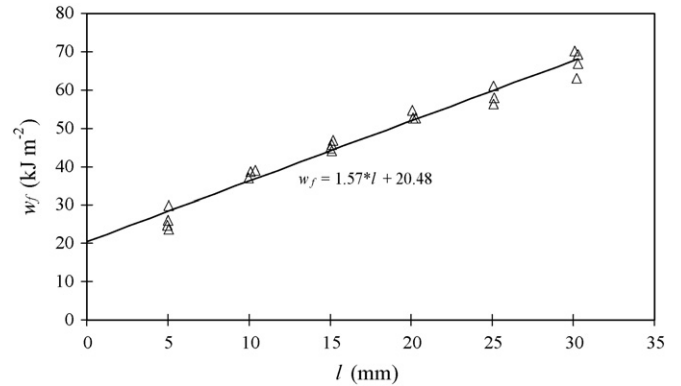


Fig. 5. Total work of fracture of NRE-211 at room temperature obtained with DENT. The specific EWF of 0.025-mm thick NRE-211 was found to be 20.5 kJ m<sup>-2</sup>.

### 3. Results and discussion

#### 3.1. DENT and trouser tear tests

Fig. 5 shows the results from DENT tests [5] and Fig. 6 shows the results from trouser tear tests [6], both conducted at ambient conditions. Because no attempt was made to determine the crack propagation rates during the DENT tests, a horizontal line is drawn to indicate how the EWF value compares to the fracture energies obtained with the trouser tear tests. It is clear that the trouser tear test effectively reduced the apparent fracture energy by nearly one order of magnitude in comparison to the DENT test for NRE-211. The decreasing trend of the trouser tear test results as cracking rate increased is somewhat abnormal. A possible reason, stick-slip was seen during tests at higher rates and the load repeatedly dropped to zero. However, being several kJ m<sup>-2</sup>, the trouser tear fracture energy

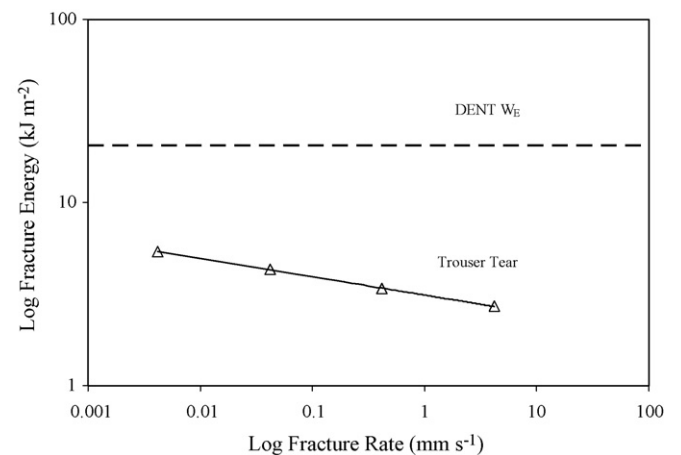


Fig. 6. Fracture energies measured with DENT and trouser tear tests at ambient conditions.

is probably one hundred times larger than the intrinsic fracture energy of the membrane [9].

### 3.2. Knife slit test

The results for the knife slit tests will be presented in two parts. The first part discusses the basic findings of the cutting and tearing energies of NRE-211 at room temperature and 40 °C, and several RH levels with a cutting angle of 30°. The second part discusses the interaction between cutting and tearing modes based on tests performed with different cutting angles and tearing weights.

Each data point in Fig. 7(a) and (b) represents the average of two or three tests conducted at a particular temperature, humidity, and cutting rate. With just a few exceptions at higher rates,

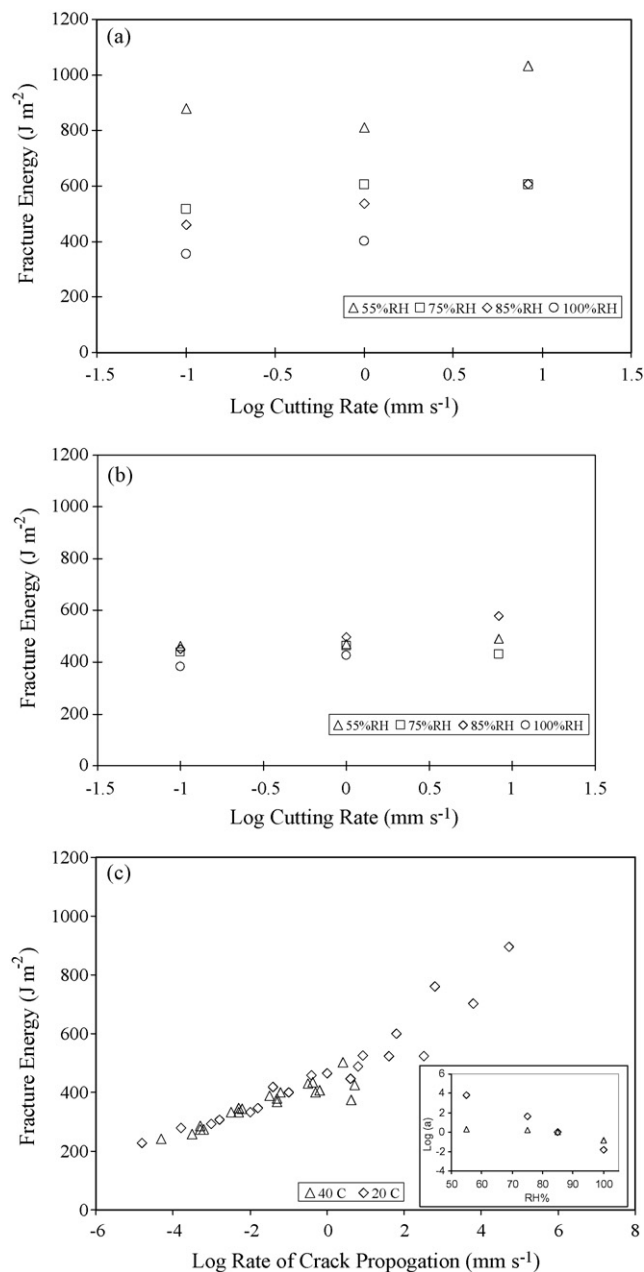


**Fig. 7.** (a) Experimental results obtained at 25 °C; (b) at 40 °C; (c) Doubly shifted hygrothermal master curve of fracture energy referenced at 25 °C and 85%RH. The inset shows the hygral shift factors at the two temperatures. To merge the data points, the temperature shift from 40 °C to 25 °C was one half logarithm decades.

the energies measured with knife slit tests are in the order of 0.15–0.6 kJ m<sup>-2</sup>. These values are much lower than those obtained with the DENT and trouser tear methods, which means much less viscous and plastic dissipations were involved in the knife slit test, significantly closing the gap between the measured fracture energy and the anticipated intrinsic fracture energy of NRE-211. Using a plane stress approximation, the plastic zone associated with the smallest measured total fracture energy ahead of the crack tip is [10]:

$$r_p \approx \frac{1}{2\pi} \left( \frac{G_{Ic} E'}{\sigma_y^2} \right) \approx \frac{1}{2\pi} \left( \frac{150 \text{ J m}^{-2} \cdot 250 \text{ MPa}}{(15 \text{ MPa})^2} \right) = 27 \mu\text{m} \quad (5)$$

which is almost equal to the thickness of the NRE-211 membrane.

After we conducted the tests at several temperatures, humidities, and fracture rates, the time–temperature–moisture superposition principle (TTMSP) was utilized to characterize the viscous dissipation. The data collected for different humidities at each temperature were first shifted horizontally toward 85%RH to form a hygral master curve. Then the hygral master curve at 40 °C was shifted one half logarithmic decade to merge with the curve at 25 °C, forming a doubly shifted hygrothermal master curve, shown in Fig. 7(c). The inset shows the hygral shift factors used at the two temperatures to form the individual hygral master curves. The humidity dependence at 25 °C is more substantial than at 40 °C. The nonzero slope of the master curve suggests that viscoelastic dissipation was still present during the tests at these two temperatures, even at the slowest rate. We are in the process of improving the environmental controlling to conduct tests at higher temperatures which will allow us to effectively cut the PEM at much lower rate in the time–temperature superposition sense, and in turn approach the membrane's intrinsic fracture energy.

Further studies were devoted to the interaction between *C* and *T* in the knife slit test. If the blade was ideally effective in eliminating viscous dissipation and plastic yielding ahead of the crack tip, and there was no frictional force between the knife and the ligaments of the specimen, then no matter how we change the cutting configuration, the total fracture energy should remain the same for a particular temperature and humidity condition. The angle dependence of the total fracture energy (in Fig. 8(a)) when there was no weight attached to the uncut ligament may be explained by reductions in frictional forces. In this sense, the bigger the cutting angle, the better is the configuration. At the same time, a bigger cutting angle means more tearing and uncontrolled plastic tearing may occur. As was discussed above, a configuration that minimizes both the frictional effects and plastic tearing is what should be sought. To investigate the plastic deformation caused by tearing (we assume the plastic zone size caused by cutting to be equal to the tip of the blade and thus negligible), three different weights were suspended under the uncut ligament to introduce varied amounts of tearing. Even the heaviest weight of 92 mN did not introduce noticeable straining of the membrane (less than 0.001, assuming an elastic modulus of 250 MPa for the PEM and at a 50° cutting angle) at the tested condition (25 °C, ambient RH), therefore the approximate equations based on negligible straining for calculating fracture energies were employed for all the tests.

In Fig. 8(b), with a suspended weight of 4.9 mN, the fracture energy first decreased with increasing cutting angle in a fashion, similar to when no tearing weight was applied, and then increased. However, it is interesting to note that the 4.9 mN tearing weight caused slight increases in the tearing energy but a noticeable decrease in the cutting energy, combining to decrease the total fracture energy. It is not completely clear how a little bit more tearing ahead of the crack tip made the membrane much easier to cut. It could be due to a decrease in the frictional force between the knife

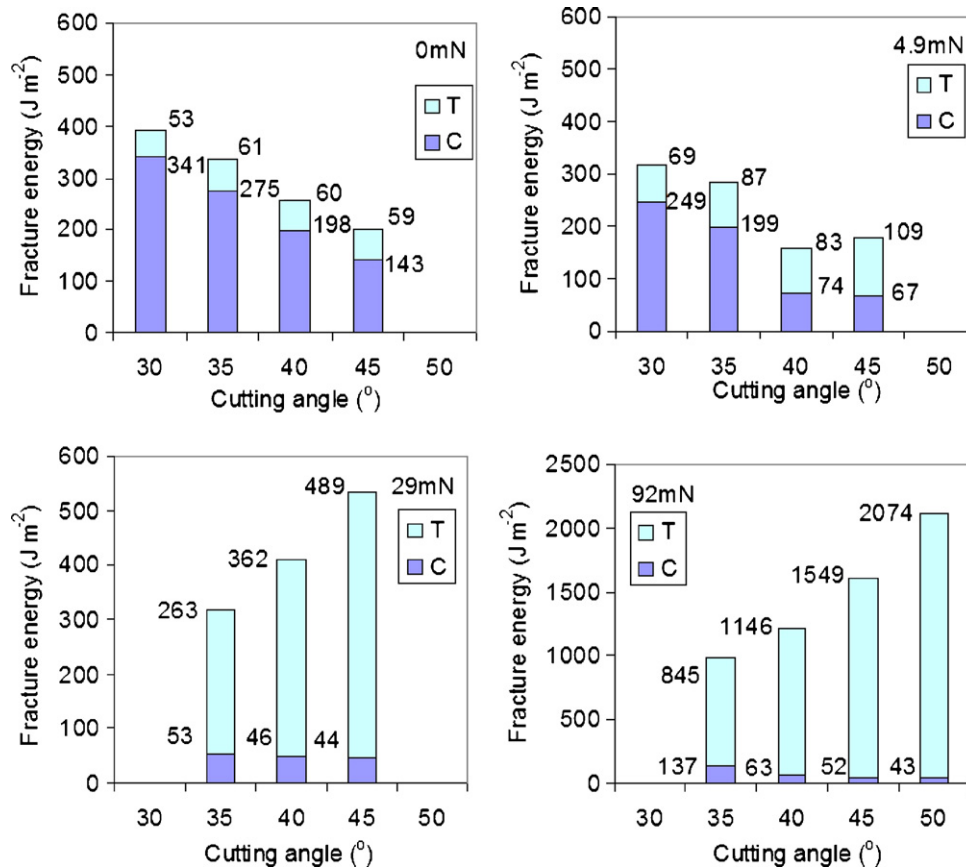


**Fig. 8.** The fracture energy varied as the cutting angle changed. When a weight was hung under the uncult ligament to introduce more tearing, the total fracture energy first dropped and then increased due to increased plastic deformation during tearing.

and the separated legs if these legs near the cutting point underwent a plate-bending to membrane-stretching transition because of the small load. Without the load, as the legs behave more like plates, the two legs are indeed parallel to each other near the blade tip; when the small load is applied and the legs behave more like membranes, the two legs are separated further near the blade tip leaving smaller contact areas. With 29 mN and 92 mN weights (in Fig. 8(c) and (d)), significant increases in tearing energy caused the total fracture energy to increase by nearly an order of magnitude. These increases suggest that too much tearing was introduced ahead of the crack tip for the sharp blade to effectively control the fracture process. All these observations are in agreement with what Gent and coworkers found [16,17]. Among the investigated combinations, the smallest total fracture energy of  $157 \text{ J m}^{-2}$  was obtained when the cutting angle was  $40^\circ$  and the tearing weight was 4.9 mN. It should be noted that such interaction between cutting and tearing energy is governed by factors including the yielding strength and energy to break of the membrane [17]. As we advance to tests at the typical operating fuel cell temperature of  $80^\circ\text{C}$  and elevated humidity, the cutting configuration that leads to the least total fracture energy could be different than the current one. A cohesive zone finite element fracture analysis of the interaction between cutting, tearing, and frictional effect could provide guidance in the search of better configurations that minimize both frictional effect and plastic deformation under different conditions.

Regardless of these complicated interactions between C and T, total fracture energies obtained with the knife slit tests at all the cutting configurations were orders of magnitude closer to the intrinsic fracture energy of the NRE-211 membrane by limiting the plastic deformation during the test. In this sense, the knife slit

test resulted in more meaningful fracture resistance information of the membrane that governs its long-term mechanical durability under sustained and/or cyclic loading, which can be caused by the hygrothermal changes between the assembly condition and the operational condition (a sustained load) and during operation at varied power levels (a cyclic load) [4,7,8].

#### 4. Concluding remarks

Fracture tests of PEM were conducted to investigate the intrinsic fracture energy of Nafion NRE-211. Knowledge of this intrinsic fracture energy can help us understand the durability of PEM and MEA when subjected to creep and/or cyclic loading conditions where they may undergo slow cracking. Because the presence of a sharp blade reduced the plastic and viscous dissipation near the crack tip in a knife slit test, the absolute values of fracture energy obtained are two orders of magnitude lower than those obtained with other common membrane fracture tests, and are just a few times the typical intrinsic fracture energy of polymers, which is on the order of  $50 \text{ J m}^{-2}$  [9]. The fact that the fracture energy still shows a rate-dependence suggests that viscous and plastic dissipation still played roles during the fracture process. Increasing the test temperature and lowering the cutting rate could further reduce viscous dissipation, better approximating the intrinsic fracture energy of the PEM, as could further studies of the interaction between cutting and tearing energies. Nonetheless, the use of the knife slit test offers considerable promise for characterizing subcritical crack growth in PEMs and MEAs, offering a new tool for investigating their durability in fuel cell environments.

## Acknowledgments

The authors are grateful to General Motors Corporation for providing support, the Department of Engineering Science and Mechanics and the Department of Mechanical Engineering for providing facilities, and the Macromolecules and Interfaces Institute at Virginia Tech for fostering interdisciplinary studies in fuel cells. JKQ thanks the National Science Foundation for the financial support received during the 2005 Summer Undergraduate Research Program at Virginia Tech (Grant No. EEC-0552738).

## References

- [1] X.Y. Huang, R. Solasi, Y. Zou, M. Feshler, K. Reifsnider, D. Condit, S. Burlatsky, T.J. Madden, J. Polym. Sci. B: Polym. Phys. 44 (2006) 2346–2357.
- [2] D. Liu, S. Kyriakides, S.W. Case, J.J. Lesko, Y.X. Li, J.E. McGrath, J. Polym. Sci. B: Polym. Phys. 44 (2006) 1453–1465.
- [3] W. Liu, K. Ruth, G. Rusch, J. New Mater. Electrochem. Syst. 4 (2001) 227–232.
- [4] Y.H. Lai, C.K. Mittelsteadt, C.S. Gittleman, D.A. Dillard, in: R.K. Shah, E.U. Ubong, S. Samuelsen (Eds.), Proceedings of the 3rd International Conference Fuel Cell Science, Engineering, and Technology, 2005, pp. 161–167.
- [5] C.S. Gittleman, M.K. Budinski, Y.H. Lai, B. Litter, D. S. Miller, Proceedings of the AIChE Annual Meetings, Austin TX, 2004.
- [6] D.A. Dillard, Y.H. Lai, M.K. Budinski, C.S. Gittleman, in: R.K. Shah, E.U. Ubong, S. Samuelsen (Eds.), Proceedings of the 3rd International Conference Fuel Cell Science, Engineering, and Technology, 2005, pp. 153–159.
- [7] R. Solasi, Y. Zou, X. Huang, K. Reifsnider, D. Condit, J. Power Sources 167 (2007) 366–377.
- [8] A. Kusoglu, A.M. Karlsson, M.H. Santare, S. Cleghorn, W.B. Johnson, J. Power Sources 170 (2007) 345–358.
- [9] G.J. Lake, A.G. Thomas, Proc. R. Soc. Lond. A: Math. Phys. Sci. 300 (1967) 108–119.
- [10] R.J. Sanford, Principles of fracture mechanics, Prentice Hall, Upper Saddle River, NJ, 2003.
- [11] J.T. Uan-Zo Li, The Effects of Structure, Humidity and Aging on the Mechanical Properties of Polymeric Ionomers for Fuel Cell Applications, Master Thesis, Virginia Polytechnic Institute and State University, Blacksburg, VA, 2001.
- [12] Y.W. Mai, B. Cotterell, Int. J. Fracture 32 (1986) 105–125.
- [13] J.S.S. Wong, D. Ferrer-Balas, R.K.Y. Li, Y.W. Mai, M.L. Maspoeh, H.J. Sue, Acta Mater. 51 (2003) 4929–4938.
- [14] ASTM International: West Conshohocken, PA, 2002.
- [15] G.J. Lake, O.H. Yeoh, Int. J. Fracture 14 (1978) 509–526.
- [16] A.N. Gent, S.M. Lai, C. Nah, C. Wang, Rubber Chem. Technol. 67 (1994) 610–618.
- [17] A.N. Gent, C. Wang, J. Polym. Sci. B: Polym. Phys. 34 (1996) 2231–2237.